

Experimental and Theoretical Studies on Organic D- π -A Systems Containing Three-Coordinate Boron Moieties as both π -Donor and π -Acceptor

Lothar Weber,*^[a] Daniel Eickhoff,^[a] Todd B. Marder,*^[b] Mark A. Fox,*^[b] Paul J. Low,^[b] Austin D. Dwyer,^[b] David J. Tozer,*^[b] Stefanie Schwedler,^[a] Andreas Brockhinke,^[a] Hans-Georg Stammler,^[a] and Beate Neumann^[a]

Abstract: Four linear π -conjugated systems with 1,3-diethyl-1,3,2-benzodiazaborolyl [$C_6H_4(NEt)_2B$] as a π -donor at one end and dimesitylboryl ($BMes_2$) as a π -acceptor at the other end were synthesized. These unusual push-pull systems contain phenylene ($-1,4-C_6H_4-$; **1**), biphenylene ($-4,4'-(1,1'-C_6H_4)_2-$; **2**), thiophene ($-2,5-C_4H_2S-$; **3**), and dithiophene ($-5,5'-(2,2'-C_4H_2S)_2-$; **4**) as π -conjugated bridges and different types of three-coordinate boron moieties serving as both π -donor and π -acceptor. Molecular structures of **2**, **3**, and **4** were determined by single-crystal X-ray diffraction. Photophysical studies on these systems reveal blue-green fluorescence in all compounds. The Stokes shifts for **1**, **2**, and **3** are notably large at $7820\text{--}9760\text{ cm}^{-1}$ in THF and $5430\text{--}6210\text{ cm}^{-1}$ in cyclohexane, whereas the Stokes shift for **4** is signifi-

cantly smaller at 5510 cm^{-1} in THF and 2450 cm^{-1} in cyclohexane. Calculations on model systems **1'**–**4'** show the HOMO to be mainly diazaborolyl in character and the LUMO to be dominated by the empty p orbital at the boron atom of the $BMes_2$ group. However, there are considerable dithiophene bridge contributions to both orbitals in **4'**. From the experimental data and MO calculations, the π -electron-donating strength of the 1,3-diethyl-1,3,2-benzodiazaborolyl group was found to lie between that of methoxy and dimethylamino groups. TD-DFT calculations on **1'**–**4'**, using B3LYP and

Keywords: charge transfer • density functional calculations • diazaborole • donor–acceptor systems • luminescence

CAM-B3LYP functionals, provide insight into the absorption and emission processes. B3LYP predicts that both the absorption and emission processes have strong charge-transfer character. CAM-B3LYP which, unlike B3LYP, contains the physics necessary to describe charge-transfer excitations, predicts only a limited amount of charge transfer upon absorption, but somewhat more upon emission. The excited-state (S_1) geometries show the borolyl group to be significantly altered compared to the ground-state (S_0) geometries. This borolyl group reorganization in the excited state is believed to be responsible for the large Stokes shifts in organic systems containing benzodiazaborolyl groups in these and related compounds.

Introduction

Three-coordinate organoboron compounds and polymers exhibit linear and nonlinear optical and electronic properties which make them attractive for use in functional materials.^[1,2] In such compounds, the three-coordinate boron center generally behaves as a π -acceptor, due to its vacant

p_z orbital, but as boron is more electropositive than carbon, the boryl moiety can also exhibit σ -donor character. The field has been dominated by the use of dimesitylboryl ($BMes_2$, Mes = 2,4,6-Me₃C₆H₂) and related moieties, as the presence of the *ortho*-methyl groups stabilizes the unsaturated boron center through steric protection of the empty p_z orbital. The $BMes_2$ group is considered to be a π -acceptor similar to NO₂ based on UV data,^[3] but closer to CN based on cyclic voltammetry (CV) data,^[4] for which reduction waves are observed. These compounds can display sizable second- and third-order nonlinear optical (NLO) properties,^[5–10] in which the $BMes_2$ acceptor strength is usually somewhere between that of NO₂ and CN. They can also exhibit large two-photon absorption (TPA) cross-sections and strong two-photon excited fluorescence (TPEF).^[11–13] Such electron-deficient compounds have low LUMO energies and have thus been shown to be efficient electron-transporting and/or -emitting layers in organic light-emitting diodes (OLEDs).^[14–16] Compounds with $BMes_2$ groups are often strongly colored and/or luminescent,^[17] and thus have potential for use as colorimetric or luminescent sensors for

[a] Prof. Dr. L. Weber, D. Eickhoff, Dr. S. Schwedler, Dr. A. Brockhinke, Dr. H.-G. Stammler, B. Neumann
Fakultät für Chemie der Universität Bielefeld
33615 Bielefeld (Germany)
E-mail: lothar.weber@uni-bielefeld.de

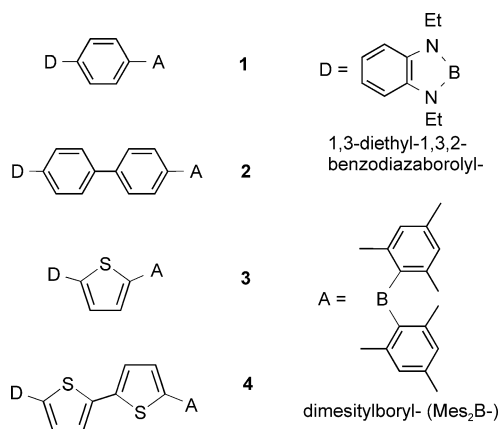
[b] Prof. Dr. T. B. Marder, Dr. M. A. Fox, Prof. Dr. P. J. Low, A. D. Dwyer, Prof. Dr. D. J. Tozer
Department of Chemistry, Durham University
Durham DH1 3LE (UK)
E-mail: todd.marder@durham.ac.uk
todd.marder@uni-wuerzburg.de
m.a.fox@durham.ac.uk
d.j.tozer@durham.ac.uk

 Supporting information for this article is available on the WWW under <http://dx.doi.org/10.1002/chem.201102059>.

anions, particularly fluoride ions.^[18,19] Conjugated molecules with boryl side groups have recently been shown to display very large Stokes shifts and high quantum yields both in solution and the solid state, properties that were attributed to the lack of close packing caused by the bulky mesityl groups.^[20,21]

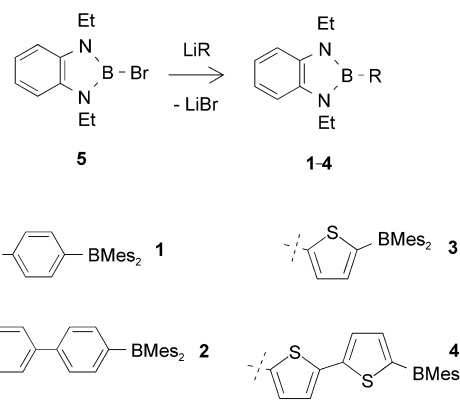
In the past decade, the chemistry of another class of three-coordinate boron compounds, namely 1,3,2-diazaboroles, has developed rapidly.^[22–27] Some of these compounds show strong fluorescence properties.^[28–36] The 1,3-diethyl-1,3,2-benzodiazaborolyl group (1,3-Et₂-1,3,2-N₂BC₆H₄) is perhaps the most widely used benzodiazaborolyl group and compounds containing this group are somewhat air-stable.^[24,30–35] Previous calculations on 2-arylethynyl-1,3,2-diazaboroles showed a localization of the HOMO on the diazaborole group, leading to the suggestion that this group could act as a π -donor.^[35] Consistent with this proposal, cyclic voltammetry studies have shown that diazaboroles oxidize easily.^[30,33,36]

As the BMes₂ group is known to be an effective π -acceptor and the benzodiazaborolyl group has been suggested to be a π -donor, the novel “push–pull” systems (**1–4**, shown here) were targeted. This study describes the syntheses, crystal structures, photophysical properties, and computational studies on these four novel compounds, each containing two different types of three-coordinate boron centers functioning as π -donor and π -acceptor. The results confirm our previous theoretical prediction of the unusual π -donor behavior of the benzodiazaborolyl moiety^[35] and provide a comparison of its donor properties with those of typical π -donor groups.



Results and Discussion

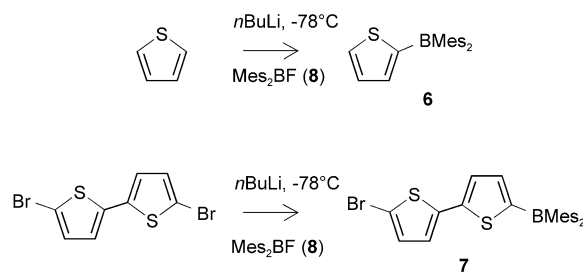
Synthesis: The new bisboryl compounds **1–4** were all formed by the established methodology^[24,25,30,31,34,35] of reacting 2-bromo-1,3-diethyl-1,3,2-benzodiazaborole^[24] (**5**) with the respective lithiated compound containing a BMes₂ group (Scheme 1). The *para*-phenylene derivative **1** was formed in 67% yield through the lithiation of 4-bromophenyldimesitylborane^[17] with *n*-butyllithium followed by addition of an



Scheme 1. General route used in the syntheses of push–pull systems **1–4**.

equimolar amount of **5**. An analogous treatment of 4'-bromobiphenyldimesitylborane^[37] with *n*-butyllithium followed by addition of **5** afforded the 4,4'-bisborylated biphenyl **2** as a colorless solid in 54% yield. The moderately air- and moisture-sensitive compounds **1** and **2** are very soluble in common organic solvents, such as benzene, ethers, CH₂Cl₂, CHCl₃, CH₃CN and DMSO.

The lithiated precursors for the syntheses of **3** and **4** were generated by reaction of 2-dimesitylborylthiophene (**6**) and 5'-bromo-5-dimesitylboryl-2,2'-dithiophene (**7**), respectively, with butyllithium. The new compounds, **6** and **7**, were obtained as oils in 59–65% yields from the reactions of dimesitylfluoroborane^[38] (Mes₂BF, **8**) with the corresponding lithiated thiophenes as shown in Scheme 2. Lithiation of **6** by *n*-butyllithium followed by addition of **5** gave **3** as an off-white solid in 67% yield. A similar procedure from **7** afforded **4** as a white solid in 71% yield.



Scheme 2. Syntheses of new dimesitylborylthiophenes **6** and **7**.

It is interesting to note that thiophenes with electron-donating amino groups, such as those in **3**, instead of the borolyl group have not yet been reported.^[15] The only reported push–pull dithiophene involving a BMes₂ group has a pyrrolidin-1-yl ((CH₂)₂N⁺) group in place of the borolyl substituent in **4**.^[10] Related systems with Ph₂N donors and B(Mes)-4-*t*BuPh or B(Mes)-4-(poly)styryl groups^[18b] as well as BPh₂ and B(C₆F₅)₂ acceptor moieties^[3b,34] have been examined previously.

X-ray structural analyses of 2, 3, and 4: The molecular structures of compounds **2**, **3**, and **4** were determined by single-crystal X-ray diffraction (Figures 1–3). Bond lengths and torsion angles of interest are listed in Table 1. The crystal structure of **2** contains three independent molecules (**2A**, **2B** and **2C**) in each unit cell; whereas for **3** there are two independ-

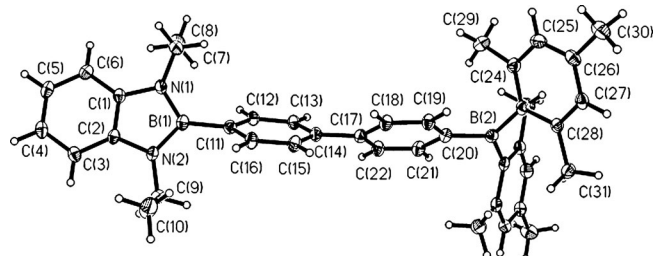


Figure 1. One of three independent molecules in the crystal structure of **2**. Ellipsoids drawn at 50 % probability. Selected bond lengths in Å: B(1)–C(11) 1.563(3); C(14)–C(17) 1.481(3); C(20)–B(2) 1.564(3). Torsion angle for C(13)–C(14)–C(17)–C(18) 39.1°.

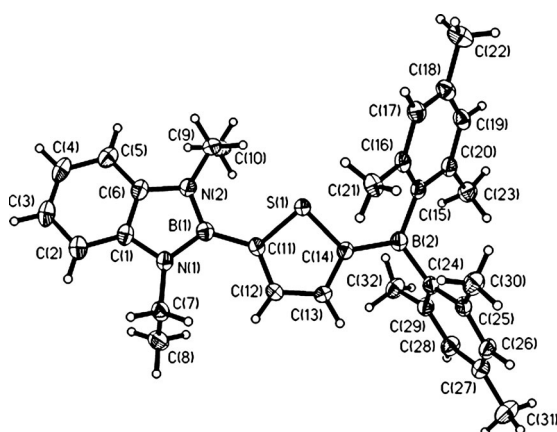


Figure 2. One of two independent molecules in the crystal structure of **3**. Ellipsoids drawn at 50 % probability. Selected bond lengths in Å: B(1)–C(11) 1.556(2); C(11)–C(12) 1.381(2); C(12)–C(13) 1.394(2); C(13)–C(14) 1.385(2); C(14)–B(2) 1.547(2).

Table 1. Selected geometric parameters for systems **2–4**.

	2A	2B	2C	3A	3B	4
bond lengths [Å]						
borolyl unit						
B–C	1.563(3)	1.566(3)	1.568(3)	1.556(2)	1.557(3)	1.561(5)
B–N	1.435(3)	1.433(3)	1.433(3)	1.438(2)	1.438(2)	1.426(5)
	1.431(3)	1.435(3)	1.434(3)	1.433(2)	1.432(2)	1.430(5)
BMes ₂ unit						
B–C	1.564(3)	1.564(3)	1.569(3)	1.547(2)	1.548(3)	1.541(5)
B–C(Mes)	1.585(3)	1.588(3)	1.586(3)	1.579(3)	1.577(3)	1.588(5)
	1.585(3)	1.586(3)	1.581(3)	1.583(3)	1.576(3)	1.577(6)
torsion angles [°]						
borolyl-C (N–B–C–C)	56.1	59.2	48.7	20.7	33.8	33.0
bridging C–BMes ₂ (C–B–C–C/S)	20.2	14.6	12.2	14.0	23.9	23.1
BMes ₂ (C–B–C–C)	54.3	56.5	55.5	54.6	50.2	56.2
	61.3	59.9	61.2	63.3	59.2	61.8
aryl–aryl	39.1	37.6	36.1			
thienyl–thienyl					168.1	

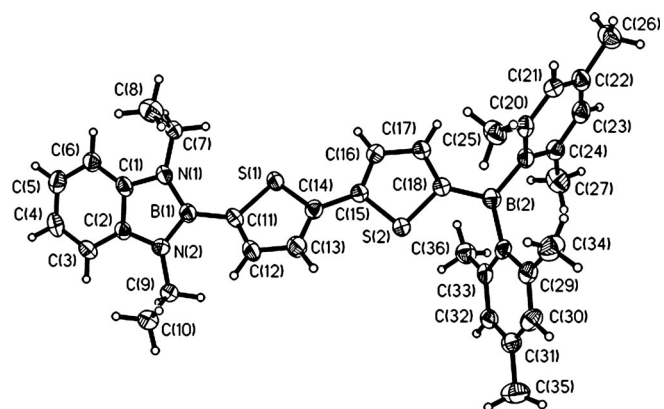


Figure 3. Molecular structure of **4**. Ellipsoids drawn at 50 % probability. Selected bond lengths in Å: B(1)–C(11) 1.561(5); C(14)–C(15) 1.473(4); C(18)–B(2) 1.541(5). Torsion angle for S(1)–C(14)–C(15)–S(2) 168.1°.

ent molecules (**3A** and **3B**). The bond lengths observed for the borolyl and BMes₂ substituents are typical of those found in crystal structures of compounds containing a benzodiazaborolyl^[24,30,35] or a BMes₂^[39,40] group.

The B–C bond lengths of the bridges shorten slightly on going from the arene bridge in **2** to the thiophene-containing bridges in **3** and **4**. Even though the mesityl groups have essentially the same twisted orientations in the solid-state structures of **2–4**, as shown by the torsion angles listed in Table 1, the bridge Mes₂B–C bond lengths are shortened by about 0.02 Å on going from the arene bridge in **2** to the thiophene bridges in **3** and **4**. This is in accord with X-ray data for Mes₂B–thiophene and Mes₂B–arene compounds reported elsewhere.^[41–44] The B–C bond lengths involving the borolyl groups are less affected by the nature of the bridge, with a range of 1.556(2) and 1.568(3) Å for **2–4**. The torsion angles between the planes of the borolyl groups and the bridges vary considerably between 20.7 and 59.2°; the measured B–C values and torsion angles are similar to those in related borolyl–thiophenes and borolyl–arenes reported elsewhere.^[31,34] The two rings in the bridges in the three conformers of **2** are not coplanar (36.1–39.1°), whereas the two thiophene rings in **4** are oriented *anti* to one another and are nearly coplanar (11.9°).

Photophysical properties: The photophysical properties of **1–4** are listed in Table 2 along with related D–π–A, D–π–D, and A–π–A systems for comparison. The lowest energy UV absorption maxima for **1–4** decrease in energy and in intensity on going from **1** to **2** to **3** to **4**, but these are not significantly influenced by different solvents. The small solvatochromic effects

Table 2. Photophysical data of **1–4** and related systems.

	Solvent	λ_{max} abs [nm]	λ_{max} abs [cm $^{-1}$]	ϵ [M $^{-1}$ cm $^{-1}$]	Solvato- chromic shift [cm $^{-1}$]	λ_{max} em [nm]	λ_{max} em [cm $^{-1}$]	Stokes shift [cm $^{-1}$]	Φ_{fl}	Solvato- chromic shift [cm $^{-1}$]	Ref.
D-π-A											
$\text{C}_6\text{H}_4(\text{NEt})_2\text{BC}_6\text{H}_4\text{BMes}_2$ 1	THF	329	30400	31600	180	477	20960	9440	0.08	3370	
	cyclohexane	327	30580	29600		408	24510	6070	0.99		
$\text{C}_6\text{H}_4(\text{NET})_2\text{B}(\text{C}_6\text{H}_4)_2\text{BMes}_2$ 2	THF	331	30210	25900	280	489	20450	9760	0.02	4330	
	cyclohexane	328	30490	23900		399	25060	5430	0.99		
$\text{C}_6\text{H}_4(\text{NET})_2\text{B}(\text{C}_4\text{H}_2\text{S})\text{BMes}_2$ 3	THF	350	28570	20100	420	482	20750	7820	0.46	1610	
	cyclohexane	345	28990	19400		439	22780	6210	0.81		
$\text{C}_6\text{H}_4(\text{NET})_2\text{B}(\text{C}_4\text{H}_2\text{S})\text{BMes}_2$ 4	THF	392	25510	32800	200	500	20000	5510	0.45	3060	
	cyclohexane	389	25710	11400		430	23260	2450	0.85		
$\text{Me}_2\text{NC}_6\text{H}_4\text{BMes}_2$	methanol	358	27930	—	400	512	19530	8400	0.05	6380	[17]
	CHCl_3	358	27930	—	400	465	21510	6420	0.26	4000	[7, 17]
	cyclohexane	353	28330	26000		386	25910	2420	0.42		[7, 17]
$\text{MeOC}_6\text{H}_4\text{BMes}_2$	CHCl_3	318	31450	—	0	372	26880	4570	—	1370	[7]
	cyclohexane	318	31450	18000		354	28250	3200	—		[7]
$\text{Me}_2\text{N}(\text{C}_6\text{H}_4)_2\text{BMes}_2$	acetonitrile	374	26740	28000	470	511	19570	8430	—		[9]
	CH_2Cl_2	376	26600		610	488	20490	6110	—		[9]
	cyclohexane	368	27210		—						[9]
D-π-D											
$\text{C}_6\text{H}_4(\text{NET})_2\text{BC}_6\text{H}_4\text{B}(\text{NET})_2\text{C}_6\text{H}_4$	THF	300	33330	20200		385	25970	7360	0.98		[34]
$\text{C}_6\text{H}_4(\text{NET})_2\text{B}(\text{C}_6\text{H}_4)_2\text{B}(\text{NET})_2\text{C}_6\text{H}_4$	THF	304	32890			427	23420	9470	0.52		[30]
$\text{C}_6\text{H}_4(\text{NET})_2\text{B}(\text{C}_4\text{H}_2\text{S})\text{B}(\text{NET})_2\text{C}_6\text{H}_4$	THF	316	31650			404	24750	6900	0.59		[30]
$\text{C}_6\text{H}_4(\text{NET})_2\text{B}(\text{C}_4\text{H}_2\text{S})_2\text{B}(\text{NET})_2\text{C}_6\text{H}_4$	THF	351	28490	33000		448	22320	6170	0.52		[34]
A-π-A											
$\text{Mes}_2\text{BC}_6\text{H}_4\text{BMes}_2$	CHCl_3	338	29590	23000		394	25380	4210	—		[2, 6]
$\text{Mes}_2\text{B}(\text{C}_6\text{H}_4)_2\text{BMes}_2$	CHCl_3	342	29240	59000		423	23640	5600	—		[2, 6]
$\text{Mes}_2\text{B}(\text{C}_4\text{H}_2\text{S})\text{BMes}_2$	THF	—	—	—		440	22730	—	—		[45]
$\text{Mes}_2\text{B}(\text{C}_4\text{H}_2\text{S})_2\text{BMes}_2$	THF	402	24880	53700		446	22420	2460	0.86		[14]

show that these systems have small dipole moments in the ground state.

All of the compounds **1–4** are luminescent; the thiophenes **3** and **4** have moderate fluorescence quantum yields of $\Phi_{\text{fl}} = 0.45$ and 0.46, respectively, in THF, whereas Φ_{fl} for the phenylenes **1** and **2** is only 0.02 and 0.08, respectively. This contrasts with reported D- π -D systems in which the quantum yields for systems containing phenylene bridges are superior to systems containing thiophene bridges in THF (Table 2). In cyclohexane, high fluorescence quantum yields of $\Phi_{\text{fl}} = 0.99$, 0.99, 0.81 and 0.85 were obtained for **1–4**, respectively. The nonradiative processes are presumably more efficient in the polar solvent, THF, than in the nonpolar solvent, cyclohexane, for **1–4**. The Stokes shifts for **1**, **2**, and **3** are large, with values of 5430–6210 cm $^{-1}$ in cyclohexane, and more modest for **4**, being 2450 cm $^{-1}$ in cyclohexane. In all cases, the Stokes shifts are significantly larger in the more polar solvent, THF, and solvatochromic shifts in the emission maxima of 1610–4330 cm $^{-1}$ are observed on changing the solvent from cyclohexane to THF. Such large Stokes shifts have been observed for related D- π -D systems in which the donor ends are borolyl groups (Table 2). It seems that large Stokes shifts are characteristic of compounds containing benzodiazaborolyl groups, whereas no large Stokes shifts were observed with A- π -A systems containing dimesitylb-

yl groups (Table 2). Interestingly, the Stokes shift generally increases on going from $(\text{C}_4\text{H}_2\text{S})_2 < (\text{C}_4\text{H}_2\text{S}) < \text{C}_6\text{H}_4 < (\text{C}_6\text{H}_4)_2$ in all D- π -A, D- π -D, and A- π -A systems listed in Table 2. The substantial solvatochromic shifts in the fluorescence data for **1–4** may indicate that the compounds have relatively large dipole moments in their singlet excited states, *vide infra*. Indeed, experimental differences between ground- and excited-state dipole moments, estimated using the Lippert–Mataga method, of 14.4 and 18.8 D have recently been reported for **3** and **4**, respectively, in a study of their solvatochromic and fluoride sensing properties.^[32] However, we note that significant solvatochromic shifts in emission spectra of the centrosymmetric *para*-disubstituted bis(1,3-diethyl-1,3,2-benzodiazaborolyl)diphenylacetylene have recently been reported.^[31] Thus, the observed emission solvatochromism may reflect factors other than just changes in dipole moments.

It is instructive to compare the photophysical data of **1** and **2** with those of $\text{Me}_2\text{NC}_6\text{H}_4\text{BMes}_2$ and $\text{Me}_2\text{N}(\text{C}_6\text{H}_4)_2\text{BMes}_2$ in order to compare the borolyl group with the strong π -donor Me_2N group. The absorption maxima in these compounds suggest that the borolyl group is a weaker π -donor group than the Me_2N group; however, the data for **1** and $\text{MeOC}_6\text{H}_4\text{BMes}_2$ imply that the borolyl group is a stronger π -donor group than the methoxy group.

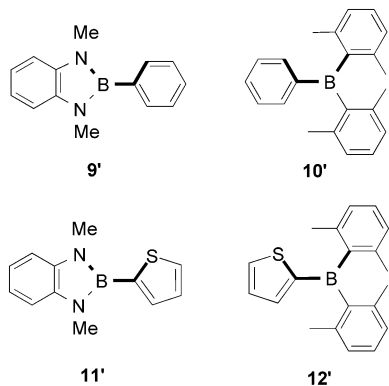
Geometry computations: Geometries of model compounds **1'-4'**, in which the ethyl groups were replaced by methyl groups and the *para*-methyl groups of the mesityl moieties were replaced by hydrogen atoms to reduce computational effort, were optimized by means of DFT calculations at the B3LYP/6-31G* level of theory. Important parameters of these optimized geometries are listed in Table 3 to compare

Table 3. Comparison of selected parameters for calculated geometries **1'-4'** and experimental (averaged) geometries **2-4**.

	1'	2	2'	3	3'	4	4'
bond lengths [Å]							
borolyl unit							
B–C	1.565	1.566	1.564	1.557	1.558	1.561	1.556
B–N	1.442	1.433	1.442	1.435	1.442	1.428	1.442
BMes ₂ unit							
B–C	1.571	1.566	1.569	1.548	1.548	1.541	1.544
B–C(Mes)	1.588	1.585	1.588	1.579	1.588	1.583	1.589
torsion angles [°]							
borolyl-C	49.7	54.7	50.2	27.3	45.1	33.0	43.3
C–BMes ₂	22.2	15.7	21.6	19.0	17.4	23.1	16.2
BMes ₂	57.4	58.1	57.4	56.8	58.6	59.0	58.8
aryl-aryl							
thienyl-thienyl						168.1	175.6

with experimental data for **2-4**. The agreements between optimized and experimental B–C bond lengths on the bridges are very good. The largest geometric differences between the optimized and experimental geometries are the torsion angles between the planes of the thiophene ring and the borolyl group in **3** and **4** by 17.8 and 10.3°, respectively. Constraining the torsion angle to 27.3° (which is the averaged experimental value for **3** in the solid-state) in **3'** and optimizing the rest of the geometry gives a structure that lies 0.5 kcal mol⁻¹ higher in energy than the minimum of **3'**. This energy difference suggests that a modest rotation barrier is present at the B–C bond between the borolyl group and the thiophene bridge.

The model compounds **9'**, **10'**, **11'**, and **12'**, shown in Scheme 3, were therefore examined to estimate the rotational energy barriers at the B–C bonds between the borolyl or



Scheme 3. Model compounds, with the torsion angles shown in bold, examined for rotation barriers at the B–C bonds.

BMes₂ group and a phenyl or thienyl group. Relative energies and B–C bond lengths with respect to the torsion angles involving the bonds viewed in bold in Scheme 3 are listed in Table S1 in the Supporting Information. The preferred conformation in all cases involves the twisting of both borolyl and BMes₂ groups with respect to the phenyl or thienyl planes. A very good agreement is found in the structural parameters between the fully optimized geometry of **10'** and the X-ray determined geometry of Mes₂BPh.^[44] The energies required for the borolyl group to become coplanar with the phenyl and thienyl groups are 6.5 and 3.0 kcal mol⁻¹, respectively. In contrast, the energies required for the BMes₂ group to become coplanar with phenyl and thienyl groups are only 1.3 and 0.3 kcal mol⁻¹, respectively.

Molecular orbital computations: To compare the frontier orbitals (HOMO, LUMO) of the π-donor and π-acceptor end groups, the geometries of C₆H₄(NEt)₂BH and HBMes₂^[40] were optimized and their MOs computed. Figure 4 shows

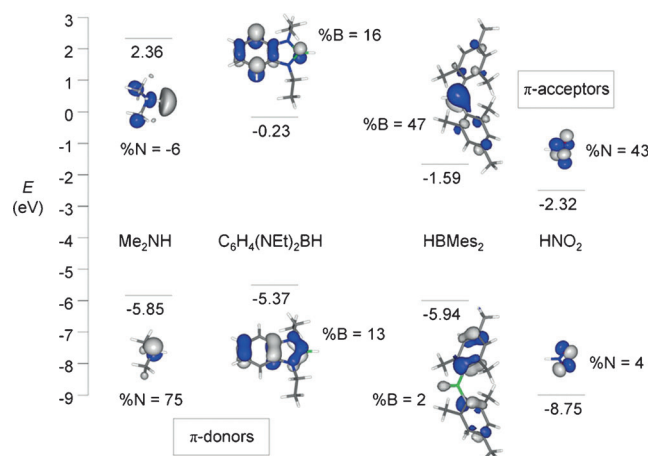


Figure 4. Comparison of frontier orbitals for Me₂NH, C₆H₄(NEt)₂BH, HBMes₂, and HNO₂.

their frontier orbitals and energies determined using B3LYP/6-31G*. The orbitals of Me₂N and NO₂ as strong π-donor and π-acceptor end groups, respectively, are also represented using Me₂NH and HNO₂ molecules for comparison. The HBMes₂ compound has 47% boron character (empty p orbital) in its LUMO reflecting the strong π-acceptor properties of the BMes₂ moiety.

The borolyl group is an electron donor based on a similar HOMO energy of C₆H₄(NEt)₂BH to that of HNMe₂. Irreversible oxidation waves have been reported from cyclic voltammetry data of some C₆H₄(NEt)₂BR systems.^[30,33] The D-π-D analogue of **2**, C₆H₄(NEt)₂B(C₆H₄C₆H₄)B(NEt)₂C₆H₄, shows an irreversible oxidation wave at 1.33 V which may be compared to that of related D-π-D biphenyls, Me₂NC₆H₄C₆H₄NMe₂ at 0.35 V^[46] and MeOC₆H₄C₆H₄OMe at 1.37 V.^[47] The CV data thus suggest that the C₆H₄(NEt)₂B unit, as an electron donor, behaves like a MeO group if attached to an aromatic ring. Some p-orbital character exists

at the B atom in the HOMO of $\text{C}_6\text{H}_4(\text{NEt})_2\text{BH}$, but it represents only 13% of the HOMO composition. The HOMO for the benzodiazaborolyl moiety is similar to the HOMO for the diazaborolyl moiety of $\text{H}_2\text{C}_2(\text{N}i\text{Bu})_2\text{BH}$.^[26] These borolyl moieties are essentially aromatic π -donors rather than a p-orbital donor such as Me_2N . The benzodiazaborolyl group can thus be regarded as a ten-electron π -donor group, isoelectronic with indole, the indenyl anion, and benzimidizolium cation. The borolyl group also contains 16% boron character (empty p orbital) in its LUMO. This borolyl group can thus bond to a fluoride anion, as has been shown experimentally for $\text{C}_6\text{H}_4(\text{NEt})_2\text{B}(\text{C}_4\text{H}_2\text{S})_n\text{H}$ ($n=1,2$),^[33] $[\{\text{C}_6\text{H}_4(\text{NEt})_2\text{B}(\text{C}_4\text{H}_2\text{S})\}_2]$ and $1,3,5\text{-}[\text{C}_6\text{H}_4(\text{NEt})_2\text{B}(\text{C}_4\text{H}_2\text{S})]_3\text{C}_6\text{H}_3$.^[32] The substantially higher energy and smaller B atom contribution in the LUMO for $\text{C}_6\text{H}_4(\text{NEt})_2\text{BH}$ compared to the LUMO for HBMe_2 indicate that the BMes_2 group in the push-pull systems **1–4** is more likely to bind to a fluoride anion than the borolyl group. This has very recently been demonstrated experimentally for compounds **3** and **4**,^[32] supporting our computational results.

The energies and compositions of the important molecular orbitals for **1–4** are listed in Tables S2–S5 in the Supporting Information, and the frontier orbitals of these systems are shown in Figures 5–8. As expected from Figure 4, the HOMOs are mainly located on the benzodiazaborolyl moiety whereas the LUMOs are situated at the BMes_2 groups. The involvement of the bridge in these HOMOs and LUMOs increases on going from **1'** to **3'** to **2'** to **4'**. The dithiophene bridge makes up 63% of the LUMO and 34% of the HOMO in the frontier orbitals for **4'**. Table 4 lists the MO energies for model compounds **1'–4'** and related D- π -A, D- π -D, and A- π -A systems to examine closely whether the

Table 4. Comparison of B3LYP/6-31G* HOMO, LUMO and HOMO-LUMO gap (HLG) energies [in eV] for model geometries of **1'–4'** and related D- π -A, D- π -D and A- π -A systems.

		LUMO	HOMO	HLG
$\text{C}_6\text{H}_4(\text{NMe})_2\text{BC}_6\text{H}_4\text{BMes}_2$	1'	−1.77	−5.37	3.60
$\text{Me}_2\text{NC}_6\text{H}_4\text{BMes}_2$		−1.24	−5.29	4.05
$\text{MeOC}_6\text{H}_4\text{BMes}_2$		−1.48	−6.00	4.52
$\text{C}_6\text{H}_4(\text{NMe})_2\text{BC}_6\text{H}_4\text{B}(\text{NMe})_2\text{C}_6\text{H}_4$		−0.71	−5.27	4.56
$\text{Mes}_2\text{BC}_6\text{H}_4\text{BMes}_2$		−2.13	−6.20	4.07
$\text{C}_6\text{H}_4(\text{NMe})_2\text{B}(\text{C}_6\text{H}_4)_2\text{BMes}_2$	2'	−1.83	−5.33	3.50
$\text{Me}_2\text{N}(\text{C}_6\text{H}_4)_2\text{BMes}_2$		−1.58	−5.06	3.48
$\text{MeO}(\text{C}_6\text{H}_4)_2\text{BMes}_2$		−1.69	−5.67	3.98
$\text{C}_6\text{H}_4(\text{NMe})_2\text{B}(\text{C}_6\text{H}_4)_2\text{B}(\text{NMe})_2\text{C}_6\text{H}_4$		−1.08	−5.26	4.18
$\text{Mes}_2\text{B}(\text{C}_6\text{H}_4)_2\text{BMes}_2$		−2.04	−6.15	4.11
$\text{C}_6\text{H}_4(\text{NMe})_2\text{B}(\text{C}_4\text{H}_2\text{S})\text{BMes}_2$	3'	−1.86	−5.40	3.54
$\text{Me}_2\text{N}(\text{C}_4\text{H}_2\text{S})\text{BMes}_2$		−1.31	−5.21	3.90
$\text{MeO}(\text{C}_4\text{H}_2\text{S})\text{BMes}_2$		−1.54	−5.80	4.26
$\text{C}_6\text{H}_4(\text{NMe})_2\text{B}(\text{C}_4\text{H}_2\text{S})\text{B}(\text{NMe})_2\text{C}_6\text{H}_4$		−0.91	−5.22	4.31
$\text{Mes}_2\text{B}(\text{C}_4\text{H}_2\text{S})\text{BMes}_2$		−2.29	−6.18	3.89
$\text{C}_6\text{H}_4(\text{NMe})_2\text{B}(\text{C}_4\text{H}_2\text{S})_2\text{BMes}_2$	4'	−2.11	−5.31	3.20
$\text{Me}_2\text{N}(\text{C}_4\text{H}_2\text{S})_2\text{BMes}_2$		−1.76	−4.86	3.10
$\text{MeO}(\text{C}_4\text{H}_2\text{S})_2\text{BMes}_2$		−1.90	−5.30	3.40
$\text{C}_6\text{H}_4(\text{NMe})_2\text{B}(\text{C}_4\text{H}_2\text{S})_2\text{B}(\text{NMe})_2\text{C}_6\text{H}_4$		−1.54	−5.11	3.57
$\text{Mes}_2\text{B}(\text{C}_4\text{H}_2\text{S})_2\text{BMes}_2$		−2.42	−5.75	3.33

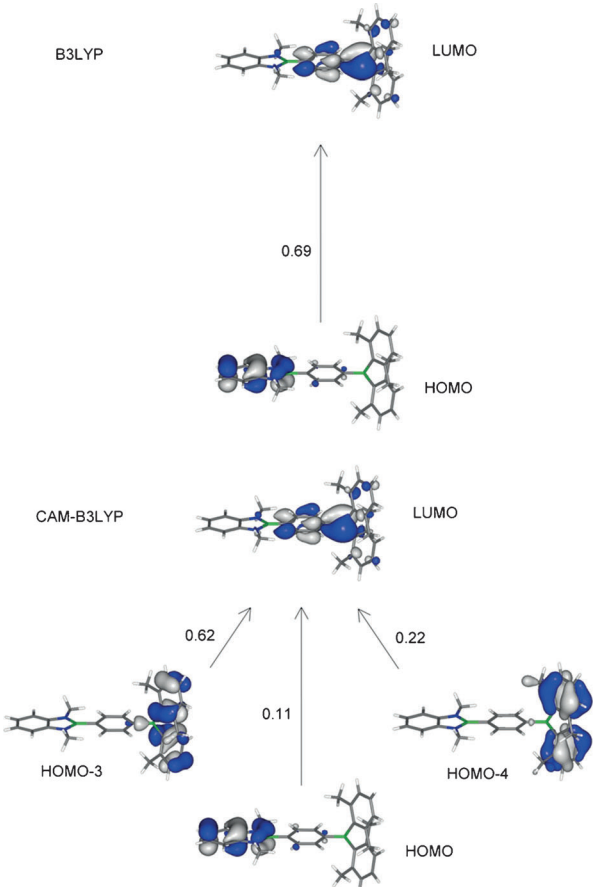


Figure 5. Orbital transitions for **1'** with corresponding κ_{ia} value for B3LYP and CAM-B3LYP functionals. MOs shown in this and subsequent figures are from B3LYP/6-31G* which are indistinguishable to MOs from CAM-B3LYP/6-31G*.

borolyl group behaves more like a MeO group or a Me_2N group when connected to different π -rings. Comparing the HOMO energies of **1'–4'** with those of the MeO and Me_2N analogues, it can be seen that the borolyl group is more like the Me_2N group for **1'**, between MeO and Me_2N for **2'** and **3'** and similar to the MeO group for **4'**. In general, the HOMO–LUMO gaps (HLG) are considerably smaller for the dithiophene systems compared to the other three.

TD-DFT computations—absorption: To provide insight into the optical absorption process, TD-DFT was used to study the lowest vertical excitation in the four models, **1'–4'**. Singlet vertical excitation energies and oscillator strengths were determined using the B3LYP and CAM-B3LYP^[48] exchange-correlation functionals at their respective ground-state geometries. B3LYP is a hybrid functional containing 20% exact orbital exchange at all interelectronic distances. It is well-established that the low percentage at large distances can lead to underestimated, spurious charge-transfer excitations.^[49] CAM-B3LYP is a Coulomb-attenuated functional, whereby the amount of exact exchange increases with interelectronic distance, to a limiting value of 65%. Studies have demonstrated that this functional provides significantly

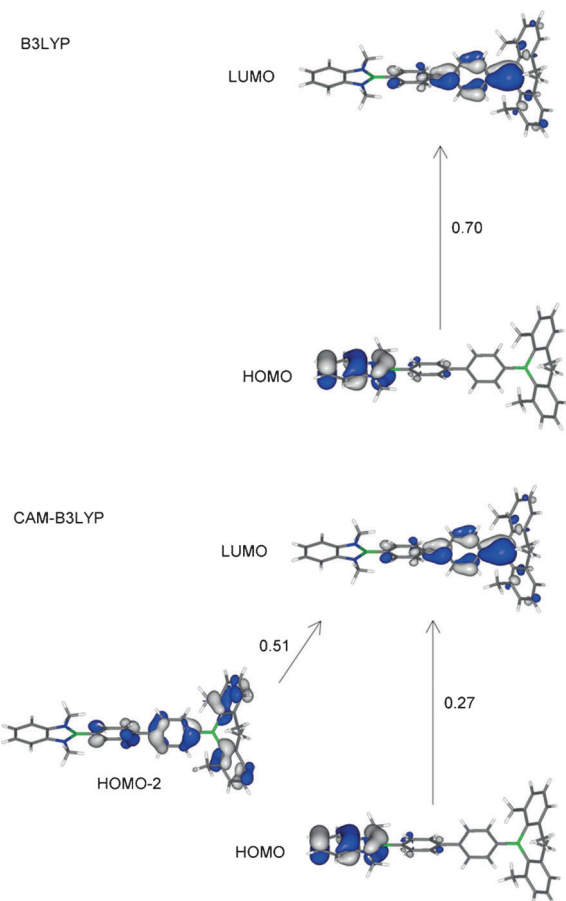


Figure 6. Orbital transitions for **2'** with corresponding κ_{ia} value for B3LYP and CAM-B3LYP functionals.

improved long-range excitation energies, such as those of charge-transfer character.^[50–56] A diagnostic test was used to help identify problematic excitations in B3LYP.^[51] The test states that when the degree of spatial overlap between the occupied and virtual orbitals involved in the excitation, as measured using a parameter Λ , is at or below approximately 0.3 for a hybrid functional, then the excitation will be significantly underestimated. Each TD-DFT excitation contains contributions from all symmetry-allowed occupied-virtual orbital pairs and the contribution of each pair was quantified using the parameter $\kappa_{ia} = X_{ia} + Y_{ia}$, in which X and Y are the solutions to the usual TD-DFT generalized Eigenvalue problem.^[57,58] Results are presented in Table 5 and dominant orbital transitions are presented in Figures 5–8.

For **1'** and **2'**, the B3LYP Λ values are only 0.31 and 0.25, respectively, and so the diagnostic test predicts that both excitation energies are unreliable. For **3'** and **4'**, the Λ values are larger, being 0.39 and 0.54, respectively, and so the diagnostic test does not predict a breakdown. Despite this, the excitations are of long-range character and so the accuracy of the B3LYP description must still be questionable. The situation somewhat resembles a study^[55] in which a long-range excitation was shown to be significantly in error, despite exhibiting a large value of Λ . For all four molecules, B3LYP

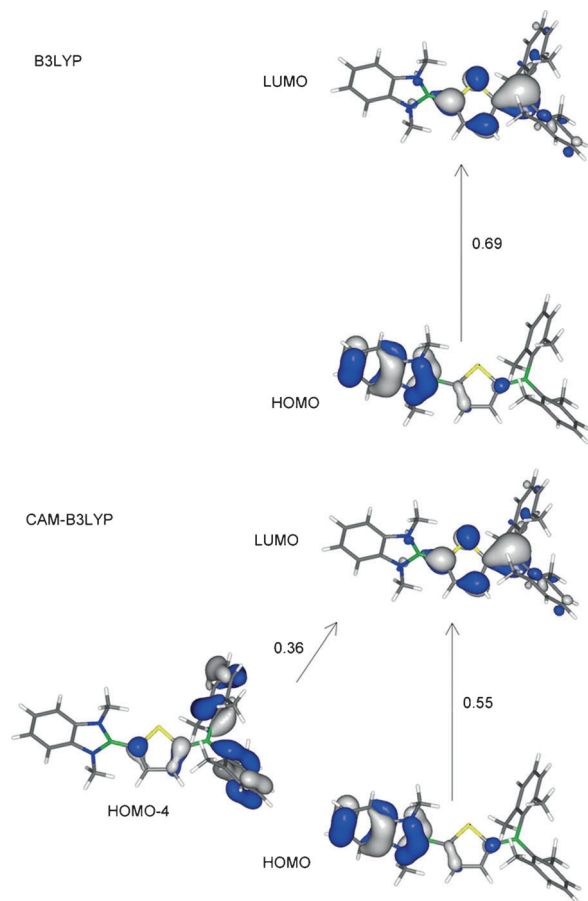


Figure 7. Orbital transitions for **3'** with corresponding κ_{ia} value for B3LYP and CAM-B3LYP functionals.

predicts that the character of the excitation is essentially pure HOMO to LUMO, as shown in Figures 5–8, indicating strong charge-transfer character. In moving to CAM-B3LYP, all excitation energies increase and, importantly, the character of the excitations change considerably, as shown in Figures 5–8. For **1'** and **2'**, the HOMO to LUMO (charge-transfer) transition still contributes, but its contribution is smaller than that of the other local transitions that do not involve the boronyl group. For **3'** and **4'**, the HOMO to LUMO transition is dominant, but there are now other significant contributions. Overall, therefore, CAM-B3LYP predicts significantly less charge-transfer character in the lowest vertical excitation than B3LYP. Given that B3LYP is known to introduce spuriously low charge-transfer states and that CAM-B3LYP contains the necessary physics (long-range exact exchange) to fix this deficiency, we suggest that the CAM-B3LYP picture is more representative of the actual absorption process. In support of this, we have performed additional high-level ab initio CCSD calculations on a simpler model system, 1-(H₂N)₂B-4-(H₂B)C₆H₄. Once again, B3LYP predicts a low Λ excitation in which a single orbital transition is dominant, whereas CAM-B3LYP predicts that additional orbital transitions are present. CCSD predicts the same picture as CAM-B3LYP.

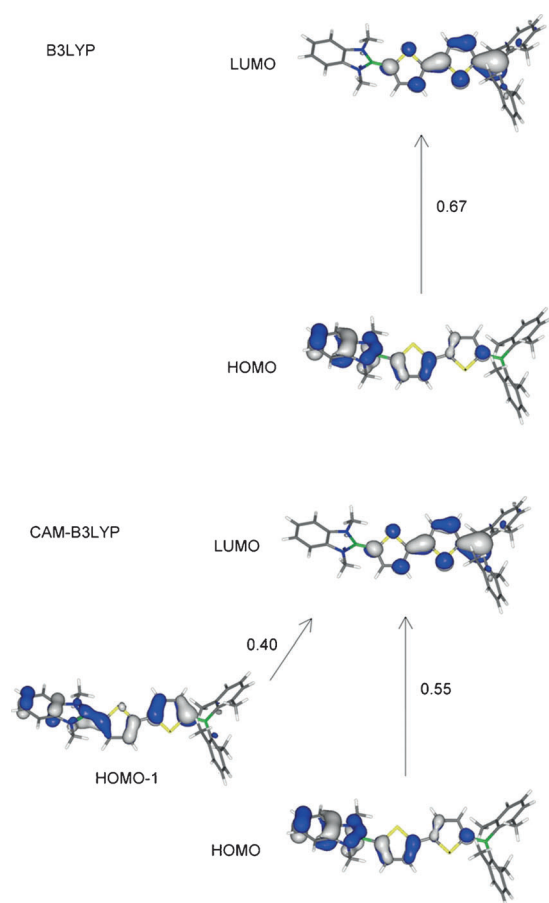


Figure 8. Orbital transitions for **4'** with corresponding κ_{ia} value for B3LYP and CAM-B3LYP functionals.

As is common in such calculations, the excitation energies in Table 5 are not strictly comparable with the λ_{\max} values, due to the presence of vibrational structure in the latter. However, it is clear that CAM-B3LYP does correctly predict the variation in the excitation energies between the four systems. In addition, while the calculations are based on static geometries, an ensemble of geometries will exist in solution, differing, for example, in the dihedral angles between rings. A barrier of about 3.8 kcal mol⁻¹ was calculated for rotation around the central thiophene–thiophene bond in the ground state of **4'**. In this regard, we note that the oscillator strengths are very sensitive to the torsion angles in molecules **2'** and **4'**.

Excited-state structures: Table 6 lists selected bond lengths and angles for the optimized (S_1) excited-state geometries for **1'-4'** at both B3LYP/6-31G* and CAM-B3LYP/6-31G* levels. Comparison of the data with the ground-state geometries in Table 3 reveals that at B3LYP/6-31G* the most significant structural changes involve the boron units. Figure 9 shows important bond lengths in the two states for **2'**. The B–C bonds are shorter by 0.04 Å, whereas the B–N bonds are longer by 0.04 Å in the boron groups for the excited-state geometries compared to the ground-state geometries in all molecules. The bridges and the BMes₂ groups are not significantly altered and the twisting angles between the donor, link, and acceptor still remain largely unchanged on going from the ground state to the excited state. Optimized excited-state geometries carried out at CAM-B3LYP/6-31G* reveal similar geometries as those from B3LYP/6-31G* for the short molecules, **1'** and **3'**, but differ for the long molecules, **2'** and **4'**. The CAM-B3LYP geometries show less twisting between the boron-containing groups and the bridges than the B3LYP geometries, but remain nonplanar.

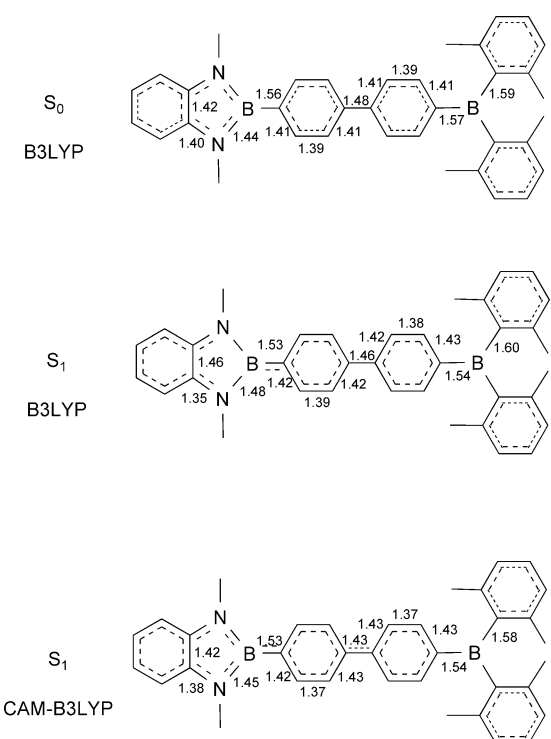
Table 5. TD-DFT data for the first vertical excitation using B3LYP and CAM-B3LYP functionals for **1'-4'**.

	Observed [eV]	B3LYP [eV]	Osc. strength [f]	Transition (κ_{ia})	CAM-B3LYP [eV]	Osc. strength [f]	Major transitions (κ_{ia})
1'	3.78	3.19	0.234	HOMO→LUMO (0.69)	4.22	0.096	HOMO→LUMO (0.11) HOMO-3→LUMO (0.62) HOMO-4→LUMO (0.22)
2'	3.78	3.19	0.274	HOMO→LUMO (0.70)	4.23	0.763	HOMO→LUMO (0.27) HOMO-2→LUMO (0.51)
2'(0)^[a]		3.10	0.343	HOMO→LUMO (0.69)	4.08	1.214	HOMO→LUMO (0.38)
2'(90)^[a]		3.37	0.004	HOMO→LUMO (0.70)	4.28	0.080	HOMO-2→LUMO (0.53) HOMO-3→LUMO (0.64)
3'	3.60	3.10	0.266	HOMO→LUMO (0.69)	4.04	0.584	HOMO→LUMO (0.55) HOMO-4→LUMO (0.36)
4'	3.19	2.85	0.677	HOMO→LUMO (0.67)	3.57	1.127	HOMO→LUMO (0.55) HOMO-1→LUMO (0.40)
4'(0)^[b]		2.84	0.619	HOMO→LUMO (0.67)	3.55	1.134	HOMO→LUMO (0.55) HOMO-1→LUMO (0.40)
4'(90)^[b]		3.14	0.005	HOMO→LUMO (0.70)	4.22	0.069	HOMO-4→LUMO (0.56) HOMO-5→LUMO (0.33)

[a] From a partly-optimized geometry with a fixed torsion angle between the two phenylene rings. [b] From a partly-optimized geometry with a fixed torsion angle between the two thiophene rings.

Table 6. Comparison of selected parameters for calculated S₁ excited-state geometries of **1'-4'**.

	1' B3LYP	1' CAM-B3LYP	2' B3LYP	2' CAM-B3LYP	3' B3LYP	3' CAM-B3LYP	4' B3LYP	4' CAM-B3LYP
bond lengths [Å]								
borolyl unit								
B–C	1.526	1.499	1.527	1.531	1.513	1.491	1.513	1.529
B–N	1.484	1.486	1.480	1.453	1.483	1.481	1.478	1.447
BMes ₂ unit								
B–C	1.556	1.533	1.541	1.541	1.544	1.523	1.528	1.532
B–C(Mes)	1.595	1.592	1.601	1.587	1.592	1.588	1.596	1.584
torsion angles [°]								
borolyl-C	58.1	31.3	46.1	35.8	38.5	19.1	30.8	29.2
C–BMes ₂	19.2	16.2	16.4	20.0	20.9	14.7	13.5	15.5
BMes ₂	54.2	55.7	57.0	53.8	56.9	59.2	60.2	59.3
aryl–aryl			21.4	10.1	52.2	55.0	57.3	54.8
thienyl–thienyl							178.8	180.0

Figure 9. Selected bond lengths of optimized geometries for **2'** at ground (**S**₀) and excited (**S**₁) states at B3LYP/6-31G*. The optimized **S**₁ geometry of **2'** at CAM-B3LYP is included for comparison.

This is consistent with the recent observation^[50] that functionals with insufficient exact exchange tend to artificially favor twisted geometries due to their increased charge-transfer character. In the CAM-B3LYP **S**₁ geometries for **2'** and **4'**, the borolyl groups do not alter geometrically compared to their respective **S**₀ geometries. The two-ring bridges, however, are flatter and have quinoidal character. The bonds linking the identical rings are 1.429 and 1.391 Å for **2'** and **4'**, respectively, compared to 1.483 and 1.447 Å for the corresponding bonds at the ground states. Figure 9 shows the bond-length differences between the B3LYP and CAM-B3LYP for the **S**₁ state of **2'**.

The link between the CAM-B3LYP excited-state geometries and the occupied molecular orbitals involved in the lowest energy CAM-B3LYP transitions for all models is revealing. Only models **2'** and **4'** contain occupied molecular orbitals involving bridge character that contribute to the transitions.

Emission and Stokes shift: To provide insight into the optical emission process, vertical excitation energies were determined from the ground to first excited state, at the optimized excited-state structure. The reverse of this process is emission, that is, fluorescence. Results of our TD-DFT calculations are presented in Table 7. Interestingly, the “emission” transitions computed using CAM-B3LYP exhibit an

Table 7. TD-DFT data using B3LYP and CAM-B3LYP functionals for **S**₁ excited-state geometries **1'-4'**.

	Observed [eV] ^[a]	B3LYP [eV]	Osc. strength [f]	Transition (κ_{ia})	CAM-B3LYP [eV]	Osc. strength [f]	Major transitions (κ_{ia})
1'	3.04	2.55	0.144	HOMO ← LUMO (0.71)	3.46	0.695	HOMO ← LUMO (0.66) HOMO ← LUMO +1 (0.15) HOMO–4 ← LUMO (0.13)
2'	3.11	2.55	0.327	HOMO ← LUMO (0.70)	3.54	1.455	HOMO ← LUMO (0.54) HOMO–2 ← LUMO (0.41) HOMO ← LUMO (0.67)
3'	2.83	2.53	0.262	HOMO ← LUMO (0.71)	3.23	0.718	HOMO–4 ← LUMO (0.14)
4'	2.89	2.38	0.703	HOMO ← LUMO (0.70)	2.96	1.248	HOMO ← LUMO (0.65) HOMO–1 ← LUMO (0.25)

[a] In cyclohexane.

increased charge-transfer character at this new geometry, with respect to that seen in absorption, in the sense that the HOMO \leftarrow LUMO transition is now dominant for all four systems. This is valid provided that the HOMO and LUMO at the excited-state geometries resemble those at the ground-state geometries.

The geometrical reorganization of the borolyl group may be responsible for the substantial Stokes shifts (0.67–0.77 eV) observed in the photophysical data for **1–3** here and in other organic systems containing borolyl groups. Observed and computed Stokes shift values are compared in Table 8. The agreement between values calculated using

Table 8. Comparison of observed and computed Stokes shifts [in eV].

	Observed ^[a]	B3LYP	CAM-B3LYP
1'	0.74	0.64	0.76
2'	0.67	0.64	0.69
3'	0.77	0.57	0.81
4'	0.30	0.47	0.61

[a] In cyclohexane.

CAM-B3LYP and observed values is very good for **1–3**, but less good for dithiophene **4**. As expected, the computed value for **4'** is quite sensitive to the thiophene–thiophene torsion angle using either functional, and a barrier of only about 3.8 kcal mol⁻¹ was calculated for rotation around the central C–C bond of **4'** in the ground state.

Dipole moments: The dipole moment differences between the ground and excited states for **3** and **4** have very recently been estimated from solvatochromic data using the Lippert–Mataga model.^[32] It is worth bearing in mind the fact that even centrosymmetric bis(benzodiazaborolyl) compounds can show strong solvatochromism in emission, *vide supra*. Notwithstanding this, we computed dipole moments for both ground and excited states of models **1'–4'**, using both B3LYP and CAM-B3LYP functionals; the values are listed in Table 9. The values labeled S₀ and S₀(S₁) are the ground-state dipole moments evaluated at the optimized ground-

state and first-excited-state structures, respectively. S₁ and S₁(S₀) are the first-excited-state dipole moments evaluated at the optimized excited-state and ground-state structures, respectively. The S₁(S₀) dipole moments computed using B3LYP/6-31G* are notably larger than those using CAM-B3LYP/6-31G*, consistent with our observation that the former theory predicts more charge-transfer character in absorption. Of interest is the fact that B3LYP predicts larger changes in dipole moment (S₁(S₀)–S₀) for the two-ring bridged systems **2'** and **4'** than for the one-ring bridged compounds **1'** and **3'**, whereas CAM-B3LYP predicts the opposite. This is clearly due to the greater bridge contributions found using the CAM-B3LYP functional. In addition, for all but **4'**, CAM-B3LYP predicts that vibrational relaxation in the S₁ excited state leads to an increase in dipole moment. This is consistent with the increased HOMO \leftarrow LUMO character computed for emission compared with that for absorption. Experimental values estimated from solution solvatochromic data are also presented, but extreme caution must be used in interpreting such values and comparing with theoretically determined quantities.

Conclusion

Four novel organic D- π -A systems containing three-coordinate boron moieties as both donor and acceptor were synthesized with benzodiazaborolyl groups as π -donors and dimesitylboryl groups as π -acceptors. The compounds are all fluorescent with large Stokes shifts up to 9800 cm⁻¹. While the electron-accepting property of the dimesitylboron group is known to be between that of the cyano and nitro group, the photophysical studies and computations show that the electron-donating effect of the benzodiazaborolyl group is between that of dimethylamino and methoxy groups. Molecular orbital calculations on these novel organic D- π -A systems show the HOMO to be mainly located on the borolyl group and the LUMO to be mainly located on the BMes₂ group, but the involvement of the π -bridge (phenylene, biphenylene, thiophene, dithiophene) between these groups in these frontier orbitals vary, being dominant in the dithiophene derivative. Insight into the absorption and emission processes is provided by TD-DFT calculations using both B3LYP and CAM-B3LYP functionals, which also allowed us to compare their behavior. B3LYP predicts that both the absorption and emission processes are strongly charge-transfer in character. CAM-B3LYP predicts only a limited amount of charge-transfer in absorption, but somewhat more in emission. CAM-B3LYP, unlike B3LYP, does contain the physics necessary to describe charge-transfer excitations. In the excited-state (S₁) geometries, the borolyl group is significantly altered compared to the ground-state (S₀) geometries. This borolyl group reorganization in the excited state is believed to be responsible for the large Stokes shifts in organic systems with benzodiazaborolyl groups reported here and elsewhere.

Table 9. Dipole moments in Debye (B3LYP/6-31G* and CAM-B3LYP/6-31G*).

	1'	2'	3'	4'
B3LYP S ₀	0.1	0.1	1.0	1.1
B3LYP S ₀ (S ₁)	0.6	0.1	1.0	1.1
B3LYP S ₁	23.7	33.3	18.4	20.7
B3LYP S ₁ (S ₀)	24.3	37.4	20.6	22.5
B3LYP S ₁ –S ₀	23.6	33.2	17.4	19.6
experimental estimate ^[a]			14.4	18.8
CAM-B3LYP S ₀	0.2	0.1	1.0	0.7
CAM-B3LYP S ₀ (S ₁)	0.4	0.2	1.1	1.0
CAM-B3LYP S ₁	14.9	9.2	11.6	6.3
CAM-B3LYP S ₁ (S ₀)	5.3	2.7	8.3	6.5
CAM-B3LYP S ₁ –S ₀	14.7	9.1	10.6	5.6
experimental estimate ^[a]			14.4	18.8

[a] Estimated from solvatochromic data using the Lippert–Mataga model.^[32]

Experimental Section

All manipulations were performed under an atmosphere of dry oxygen-free argon using Schlenk techniques. All solvents were dried with the usual drying agents and then freshly distilled prior to use. The compounds 4-bromophenyldimesitylborane,^[17] 2-bromo-1,3-diethyl-1,3,2-benzodiazaborole (**5**),^[24] 4'-bromo-4-dimesitylboryl-biphenyl,^[37] dimesitylfluoroborane (**8**),^[38] and 5,5'-dibromodithiophene^[60] were prepared according to literature methods, and 4,4'-dibromobiphenyl and 1,4-dibromobenzene were purchased from Acros. NMR spectra were recorded from solutions at room temperature in C₆D₆ or CDCl₃ (unless otherwise stated) on a Bruker AM Avance DRX500 spectrometer (¹H, ¹¹B, ¹³C) with SiMe₄ (¹H, ¹³C) and BF₃OEt₂ (¹¹B) as external standards. Some expected broad ¹³C peaks corresponding to the carbon attached to boron were not detected above the noise levels. Mass spectra were obtained with a VG Autospec sector field mass spectrometer (Micromass). For detailed spectroscopic data see the Supporting Information. Absorption spectra were measured with a UV/VIS double-beam spectrometer (Shimadzu UV-2550). For details see the Supporting Information.

4-(Dimesitylboryl)-1-(1',3'-diethyl-1',3',2'-benzodiazaborol-2'-yl)benzene

(1): A solution of 1.6 M *n*-butyllithium (1.90 mL, 3.04 mmol) in *n*-hexane was added to a solution (−78 °C) of (4-bromophenyl)(dimesityl)borane (0.79 g, 2.95 mmol) in THF (25 mL). The mixture was stirred 1 h at −78 °C before a sample of neat **5** (0.75 g, 2.96 mmol) was added. The reaction mixture was warmed to ambient temperature with stirring for 16 h. Solvent and volatile components were removed in vacuo. The solid residue was triturated three times with boiling *n*-hexane. The filtrate was evaporated to dryness and the residue was crystallized from *n*-hexane to afford a colorless microcrystalline solid **1** (0.99 g, 67% yield). Elemental analysis calcd (%) for C₃₄H₄₀B₂N₂: C 81.95, H 8.09, N 5.62; found: C 81.89, H 7.99, N 5.43.

4'-Dimesitylboryl-4-(1'',3'',2''-benzodiazaborole-2''-yl)-biphenyl (2): A solution of 1.6 M *n*-butyllithium (2.40 mL, 3.84 mmol) in *n*-hexane was added to a solution (−78 °C) of 4'-bromo-4-dimesitylborylbiphenyl (1.80 g, 3.74 mmol) in THF (40 mL). The mixture was stirred 1 h at −78 °C before a sample of neat **5** (0.97 g, 3.84 mmol) was added. Stirring was continued for 1 h at −78 °C and for 16 h at room temperature. After evaporation to dryness the residue was suspended in toluene (30 mL) and the obtained slurry was filtered. The filtrate was concentrated and stored at −35 °C for 2 d and a colorless microcrystalline product **2** was obtained (1.16 g, 54% yield). Elemental analysis calcd (%) for C₄₀H₄₄B₂N₂·0.5CH₂Cl₂: C 74.69, H 7.03, N 4.25; found: C 74.98; H 7.30, N 4.14.

2-Dimesitylboryl-5-(1',3',2'-benzodiazaborol-2'-yl)-thiophene (3): A solution of 1.6 M *n*-butyllithium (1.75 mL, 2.81 mmol) in *n*-hexane was added to a solution (−78 °C) of 2-dimesitylborylthiophene (**6**) (0.85 g, 2.56 mmol) in THF (40 mL). Stirring was continued for 15 min and for another 60 min at ambient temperature. The reaction mixture was re-cooled to −78 °C and then neat **5** (0.65 g, 2.56 mmol) was added. The solution was warmed to room temperature and stirred for 6 h. After removing solvent and volatile components in vacuo, the remaining green oil was purified by short-path distillation (350 °C, 10^{−6} bar) to give an off-white solid. Recrystallization of the solid from *n*-pentane at −35 °C gave colorless crystals of **3** (0.80 g, 67% yield). Elemental analysis calcd (%)

for C₃₂H₃₈B₂N₂S: C 76.21, H 7.59, N 5.55; found: C 76.09, H 7.73, N 5.50.

5-(Dimesitylboryl)-5'-(1'',3'',2''-benzodiazaborol-2''-yl)-2,2'-dithiophene (4): A solution of 1.6 M *n*-butyllithium (1.79 mL, 2.87 mmol) in *n*-hexane was added to a chilled solution (−78 °C) of **7** (1.35 g, 2.74 mmol) in *n*-hexane (30 mL). After stirring for 30 min, the mixture was warmed to ambient temperature and stirring was pursued for another 3 h. A sample of neat **5** (0.69 g, 2.74 mmol) was added and stirring of the mixture was continued for 16 h at 20 °C. The resulting slurry was filtered, and the filtrate was freed from solvent and volatile components in vacuo. The solid residue was dissolved in a minimum amount of boiling *n*-hexane and after cooling to room temperature, the solution was stored overnight at −35 °C to give a yellow solid **4** (1.34 g, 71% yield). Elemental analysis calcd (%) for C₃₆H₄₀B₂N₂S₂: C 73.73, H 6.87, N 4.78; found: C 73.68, H 6.74, N 4.60.

2-Dimesitylborylthiophene (6): A solution of 1.6 M *n*-butyllithium (4.33 mL, 6.93 mmol) in *n*-hexane was added to a solution of thiophene (0.53 g, 6.30 mmol) in THF (30 mL) at −78 °C. The mixture was warmed to 20 °C and stirred for 1 h before a solution of **8** (1.69 g, 6.30 mmol) in THF (20 mL) was added. After stirring over night, the solution was washed with water (100 mL) and the aqueous phase was extracted with diethyl ether. (2 × 100 mL). The combined organic fractions were dried over anhydrous Na₂SO₄ and volatiles were removed in vacuo. The remaining oil was purified by column chromatography at silica gel, and **6** were obtained as colorless oil (1.23 g, 59% yield). Compound **6** was identified by ¹H and ¹¹B NMR spectroscopy.

5-Bromo-5'-dimesitylboryl-2,2'-dithiophene (7): A solution 1.6 M *n*-butyllithium (2.9 mL, 4.7 mmol) in *n*-hexane was added dropwise to a solution of 5,5'-dibromo-2,2'-dithiophene (1.34 g, 4.24 mmol) in THF (40 mL) at −78 °C and the resulting mixture was then stirred for 30 min. The mixture was warmed to room temperature, stirred for 1 h and then cooled to −78 °C. Then a solution of **8** (1.11 g, 4.24 mmol) in *n*-pentane (30 mL) was added and the mixture was warmed to 20 °C. After stirring overnight, the reaction mixture was added to water (100 mL), the organic layer was separated and the aqueous layer was washed with diethyl ether (2 × 200 mL). The combined organic extracts were dried over anhydrous Na₂SO₄. The solvents were removed in vacuo. The crude residue was purified by column chromatography on silica gel with cyclohexane to afford

Table 10. Crystallographic data for compounds **2**, **3**, and **4**.

	2	3	4
formula	C ₄₀ H ₄₄ B ₂ N ₂ CH ₂ Cl ₂	C ₃₂ H ₃₈ B ₂ N ₂ S	C ₃₆ H ₄₀ B ₂ N ₂ S ₂
M _r [g mol ^{−1}]	659.32	504.32	586.44
crystal size [mm]	0.30 × 0.26 × 0.24	0.16 × 0.12 × 0.04	0.30 × 0.16 × 0.05
crystal system	monoclinic	triclinic	orthorhombic
space group	P2 ₁ /n	P̄I	Pna ₂ ₁
<i>a</i> [Å]	9.6086(2)	9.1341(2)	35.908(11)
<i>b</i> [Å]	36.0766(7)	16.4987(4)	11.664(5)
<i>c</i> [Å]	31.4181(6)	19.1034(4)	7.749(3)
<i>α</i> [°]	90	89.1668(12)	90
<i>β</i> [°]	95.3049(6)	88.3439(12)	90
<i>γ</i> [°]	90	89.5897(13)	90
<i>V</i> [Å ³]	10844.3(4)	2877.32(11)	3246(2)
<i>Z</i>	12	4	4
ρ _{calcd} [g cm ^{−3}]	1.212	1.164	1.200
μ [nm ^{−1}]	0.211	0.136	0.192
<i>F</i> (000)	4200	1080	1248
θ [°]	3.0–25.0	3.0–27.5	3.2–27.5
reflns collected	93 795	62 524	31 152
unique reflns	19 032	13 184	7 028
<i>R</i> (int)	0.040	0.049	0.1133
reflns observed [<i>I</i> > 2σ(<i>I</i>)]	15 447	9643	4142
parameters	1299	683	387
GOF	1.025	1.025	1.014
<i>R</i> _f [<i>I</i> > 2σ(<i>I</i>)]	0.0501	0.0479	0.0594
w <i>R</i> _f (all data)	0.1358	0.1248	0.1297
Δρ _{max/min} [e Å ^{−3}]	0.899/−0.633	0.276/−0.309	0.322/−0.236

7 as a light yellow oil (1.35 g, 67% yield). Compound 7 was identified by ^1H and ^{11}B NMR spectroscopy.

Computational studies: All ab initio computations at B3LYP^{[61–63]/6-31G*}^[64] level were carried out with the Gaussian 03 package.^[65] The Gaussian 09 package^[66] was used for CAM-B3LYP^{[48]/6-31G*} computations. The model and full geometries discussed herein were optimized at B3LYP/6-31G* level with no symmetry constraints, or partially optimized with a constrained dihedral angle using the keyword OPT(Z-MAT). Frequency calculations carried out on these fully optimized geometries showed no imaginary frequencies. The electronic structure and TD-DFT computations were also carried out at the same level of theory. In addition, TD-DFT computations at CAM-B3LYP^{[48]/6-31G*} were carried out on starting B3LYP/6-31G* geometries. Each TD-DFT excitation contains contributions from all symmetry-allowed occupied-unoccupied orbital pairs and the contribution of each pair was quantified using the parameter $\kappa_{ia} = X_{ia} + Y_{ia}$, in which X and Y are the solutions to the usual TD-DFT generalized Eigenvalue (TD-DFT)^[57,58] problem. The MO diagrams and orbital contributions were generated with the aid of Gabedit^[67] and GaussSum^[68] packages, respectively. Ground-state dipole moments were determined in the conventional manner, as the expectation value of the dipole operator using the ground-state density. For excited states, the dipole moments were determined as energy derivatives.

晶格数据是用一个Nonius Kappa CCD衍射计以Mo $K\alpha$ 辐射(石墨单色器, $\lambda=0.71073 \text{ \AA}$)在100 K获得的。晶格程序用于结构解决和精炼是SHELXS-97和SHELXL-97。^[69] 结构通过直接方法解决并使用全矩阵最小二乘法求得, 使用各向异性热参数对所有非氢原子进行精炼。氢原子在计算位置中包括, 具有 $U(\text{H})=1.2 U_{\text{eq}}$ 对于CH₂组和 $U(\text{H})=1.5 U_{\text{eq}}$ 对于CH₃组。晶格数据对于化合物在表10。CCDC-832085 (**2**), CCDC-832086 (**3**), 和CCDC-832087 (**4**)包含补充晶格数据。这些数据可以从剑桥晶格数据中心免费获得, 通过www.ccdc.cam.ac.uk/data_request/cif。

Acknowledgements

We thank Durham University for access to its High Performance Computing facility and the Deutsche Forschungsgemeinschaft, Bonn, Germany for financial support. T.B.M. thanks the Alexander von Humboldt Stiftung for a Research Award and the Royal Society for a Wolfson Research Merit Award. We thank Dr. Michael J. G. Peach for helpful discussions on the calculation of excited-state dipole moments.

- [1] a) C. D. Entwistle, T. B. Marder, *Angew. Chem.* **2002**, *114*, 3051–3056; *Angew. Chem. Int. Ed.* **2002**, *41*, 2927–2931; *Angew. Chem. Int. Ed.* **2002**, *41*, 2927–2931; b) Y. Shirota, *J. Mater. Chem.* **2000**, *10*, 1–25; c) S. Yamaguchi, A. Wakamiya, *Pure Appl. Chem.* **2006**, *78*, 1413–1424; d) F. Jäkle, *Coord. Chem. Rev.* **2006**, *250*, 1107–1121; e) M. Elbing, G. C. Bazan, *Angew. Chem.* **2008**, *120*, 846–850; *Angew. Chem. Int. Ed.* **2008**, *47*, 834–838; f) T. W. Hudnall, C.-W. Chiu, F. P. Gabbaï, *Acc. Chem. Res.* **2009**, *42*, 388–397; g) N. Matsumi, Y. Chujo, *Polym. J.* **2008**, *40*, 77–89; h) Z. M. Hudson, S. Wang, *Acc. Chem. Res.* **2009**, *42*, 1584–1596.
- [2] C. D. Entwistle, T. B. Marder, *Chem. Mater.* **2004**, *16*, 4574–4585.
- [3] a) M. E. Glogowski, J. L. R. Williams, *J. Organomet. Chem.* **1981**, *218*, 137–146; b) for a comparison of BPh_2 and $\text{B}(\text{C}_6\text{F}_5)_2$ acceptors, see: A. Sundararaman, R. Varughese, H. Li, L. N. Zakharov, A. L. Rheingold, F. Jäkle, *Organometallics* **2007**, *26*, 6126–6131.
- [4] A. Schulz, W. Kaim, *Chem. Ber.* **1989**, *122*, 1863–1868.
- [5] a) Z. Yuan, N. J. Taylor, T. B. Marder, I. D. Williams, S. K. Kurtz, L.-T. Cheng, *J. Chem. Soc. Chem. Commun.* **1990**, 1489–1492; b) Z. Yuan, N. J. Taylor, T. B. Marder, I. D. Williams, S. K. Kurtz, L.-T. Cheng, *Organic Materials for Non-linear Optics II* (Eds.: R. A. Hann, D. Bloor), RSC, Cambridge, **1991**, pp. 190–196; c) M. Lequan, R. M. Lequan, K. Chane-Ching, M. Barzoukas, A. Fort, H. Lahouche, G. Bravic, D. Chasseau, J. Gaultier, *J. Mater. Chem.* **1992**, *2*, 719–725; d) M. Lequan, R. M. Lequan, K. Chane-Ching, A.-C. Callier, M. Barzoukas, A. Fort, *Adv. Mater. Opt. Electron.* **1992**, *1*, 243; e) Z. Yuan, N. J. Taylor, Y. Sun, T. B. Marder, I. D. Williams, L.-T. Cheng, *J. Organomet. Chem.* **1993**, *449*, 27–37; f) Y. Liu, X. Xu, F. Zheng, Y. Cui, *Angew. Chem.* **2008**, *120*, 4614–4617.
- [6] Z. Yuan, N. J. Taylor, R. Ramachandran, T. B. Marder, *Appl. Organomet. Chem.* **1996**, *10*, 305–316.
- [7] Z. Yuan, C. D. Entwistle, J. C. Collings, D. Albesa-Jové, A. S. Batsanov, J. A. K. Howard, H. M. Kaiser, D. E. Kaufmann, S.-Y. Poon, W.-Y. Wong, C. Jardin, S. Fatallah, A. Boucekkine, J.-F. Halet, T. B. Marder, *Chem. Eur. J.* **2006**, *12*, 2758–2771.
- [8] Z. Yuan, J. C. Collings, N. J. Taylor, T. B. Marder, C. Jardin, J.-F. Halet, *J. Solid State Chem.* **2000**, *154*, 5–12.
- [9] M. Lequan, R. M. Lequan, K. Chane-Ching, *J. Mater. Chem.* **1991**, *1*, 997–999.
- [10] C. Branger, M. Lequan, R. M. Lequan, M. Barzoukas, A. Fort, *J. Mater. Chem.* **1996**, *6*, 555–558.
- [11] Z.-Q. Liu, Q. Fang, D. Wang, G. Xue, W.-T. Yu, Z.-S. Shao, M.-H. Jiang, *Chem. Commun.* **2002**, 2900–2901.
- [12] Z.-Q. Liu, Q. Fang, D. Wang, D.-X. Cao, G. Xue, W.-T. Yu, H. Lei, *Chem. Eur. J.* **2003**, *9*, 5074–5084.
- [13] a) D.-X. Cao, Z.-Q. Liu, Q. Fang, G.-B. Xu, G. Xue, G.-Q. Liu, W.-T. Yu, *J. Organomet. Chem.* **2004**, *689*, 2201–2206; b) Z.-Q. Liu, Q. Fang, D.-X. Cao, D. Wang, G.-B. Xu, *Org. Lett.* **2004**, *6*, 2933–2936; c) Z.-Q. Liu, M. Shi, F.-Y. Li, Q. Fang, Z.-H. Chen, T. Yi, C.-H. Huang, *Org. Lett.* **2005**, *7*, 5481–5484; d) M. Charlott, L. Porrès, C. D. Entwistle, A. Beeby, T. B. Marder, M. Blanchard-Desce, *Phys. Chem. Chem. Phys.* **2005**, *7*, 600–606; e) L. Porrès, M. Charlott, C. D. Entwistle, A. Beeby, T. B. Marder, M. Blanchard-Desce, *Proc. SPIE-Int. Soc. Opt. Eng.* **2005**, *5934*, 92–103; f) D.-X. Cao, Z.-Q. Liu, G.-Z. Li, G.-Q. Liu, G.-H. Zhang, *J. Mol. Struct.* **2008**, *874*, 46–50; g) J. C. Collings, S.-Y. Poon, C. Le Droumaguet, M. Charlott, C. Katan, L.-O. Pálsson, A. Beeby, J. A. Mosely, H. M. Kaiser, D. Kaufmann, W.-Y. Wong, M. Blanchard-Desce, T. B. Marder, *Chem. Eur. J.* **2009**, *15*, 198–208; h) C. D. Entwistle, J. C. Collings, A. Steffen, L.-O. Pálsson, A. Beeby, D. Albesa-Jové, J. M. Burke, A. S. Batsanov, J. A. K. Howard, J. A. Mosely, S.-Y. Poon, W.-Y. Wong, F. Ibersiene, S. Fatallah, A. Boucekkine, J.-F. Halet, T. B. Marder, *J. Mater. Chem.* **2009**, *19*, 7532–7544.
- [14] a) T. Noda, Y. Shirota, *J. Am. Chem. Soc.* **1998**, *120*, 9714–9715; b) T. Noda, H. Ogawa, Y. Shirota, *Adv. Mater.* **1999**, *11*, 283–285.
- [15] W.-L. Jia, D.-R. Bai, T. McCormick, Q.-D. Liu, M. Motala, R.-Y. Wang, C. Seward, Y. Tao, S. Wang, *Chem. Eur. J.* **2004**, *10*, 994–1006.
- [16] a) T. Noda, Y. Shirota, *J. Lumin.* **2000**, *87*–*89*, 1168–1170; b) Y. Shirota, M. Kinoshita, T. Noda, K. Okumoto, T. Ohara, *J. Am. Chem. Soc.* **2000**, *122*, 11021–11022; c) M. Kinoshita, N. Fujii, T. Tsukaki, Y. Shirota, *Synth. Met.* **2001**, *121*, 1571–1572; d) H. Doi, M. Kinoshita, K. Okumoto, Y. Shirota, *Chem. Mater.* **2003**, *15*, 1080–1089; e) W.-L. Jia, X. D. Feng, D.-R. Bai, Z. H. Lu, S. Wang, G. Vamvounis, *Chem. Mater.* **2005**, *17*, 164–170; f) W.-L. Jia, M. J. Moran, Y.-Y. Yuan, Z. H. Lu, S. Wang, *J. Mater. Chem.* **2005**, *15*, 3326–3333; g) M. Mazzeo, V. Vitale, F. Della Sala, M. Anni, G. Barbarella, L. Favaretto, G. Sotgiu, R. Cingolani, G. Gigli, *Adv. Mater.* **2005**, *17*, 34–39; h) W.-Y. Wong, S.-Y. Poon, M.-F. Lin, W.-K. Wong, *Aust. J. Chem.* **2007**, *60*, 915–922; i) G.-J. Zhou, C.-L. Ho, W.-Y. Wong, Q. Wang, D.-G. Ma, L.-X. Wang, Z.-Y. Lin, T. B. Marder, A. Beeby, *Adv. Funct. Mater.* **2008**, *18*, 499–511.
- [17] J. C. Doty, B. Babb, P. J. Grisdale, M. E. Glogowski, J. L. R. Williams, *J. Organomet. Chem.* **1972**, *38*, 229–236.
- [18] a) S. Yamaguchi, S. Akiyama, K. Tamao, *J. Am. Chem. Soc.* **2001**, *123*, 11372–11375; b) S. Yamaguchi, T. Shirasaka, S. Akiyama, K. Tamao, *J. Am. Chem. Soc.* **2002**, *124*, 8816–8817; c) Y. Kubo, M. Yamamoto, M. Ikeda, M. Takeuchi, S. Shinkai, S. Yamaguchi, *Angew. Chem.* **2003**, *115*, 2082–2086; *Angew. Chem. Int. Ed.* **2003**, *42*, 2036–2040; d) S. Solé, F. P. Gabbaï, *Chem. Commun.* **2004**, 1284–1285;

- e) M. Melaïmi, F. P. Gabbaï, *J. Am. Chem. Soc.* **2005**, *127*, 9680–9681; f) A. Sundararaman, M. Victor, R. Varughese, F. Jäkle, *J. Am. Chem. Soc.* **2005**, *127*, 13748–13749; g) T. W. Hudnall, M. Melaïmi, F. P. Gabbaï, *Org. Lett.* **2006**, *8*, 2747–2749; h) K. Parab, K. Venkatasubbiah, F. Jäkle, *J. Am. Chem. Soc.* **2006**, *128*, 12879–12885; i) C.-W. Chiu, F. P. Gabbaï, *J. Am. Chem. Soc.* **2006**, *128*, 14248–14249; j) E. Sakuda, A. Funahashi, N. Kitamura, *Inorg. Chem.* **2006**, *45*, 10670–10677; k) D.-R. Bai, X.-Y. Liu, S. Wang, *Chem. Eur. J.* **2007**, *13*, 5713–5723; l) S.-B. Zhao, T. McCormick, S. Wang, *Inorg. Chem.* **2007**, *46*, 10965–10967; m) M. H. Lee, T. Agou, J. Kobayashi, T. Kawashima, F. P. Gabbaï, *Chem. Commun.* **2007**, 1133–1135; n) X.-Y. Liu, D.-R. Bai, S. Wang, *Angew. Chem.* **2006**, *118*, 5601–5604; *Angew. Chem. Int. Ed.* **2006**, *45*, 5475–5478; o) M.-S. Yuan, Z.-Q. Liu, Q. Fang, *J. Org. Chem.* **2007**, *72*, 7915–7922.
- [19] T. W. Hudnall, F. P. Gabbaï, *J. Am. Chem. Soc.* **2007**, *129*, 11978–11986.
- [20] a) C.-H. Zhao, A. Wakamiya, Y. Inukai, S. Yamaguchi, *J. Am. Chem. Soc.* **2006**, *128*, 15934–15935; b) H. Li, K. Sundararaman, K. Venkatasubbiah, F. Jäkle, *J. Am. Chem. Soc.* **2007**, *129*, 5792–5793.
- [21] A. Wakamiya, K. Mori, S. Yamaguchi, *Angew. Chem.* **2007**, *119*, 4351–4354; *Angew. Chem. Int. Ed.* **2007**, *46*, 4273–4276.
- [22] a) L. Weber, *Coord. Chem. Rev.* **2001**, *215*, 39–77; b) L. Weber, *Coord. Chem. Rev.* **2008**, *252*, 1–31.
- [23] a) M. Yamashita, K. Nozaki, *J. Synth. Org. Chem. Jpn.* **2010**, *68*, 359–369; b) M. Yamashita, K. Nozaki, *Pure Appl. Chem.* **2008**, *80*, 1187–1194; c) M. Yamashita, K. Nozaki, *Bull. Chem. Soc. Jpn.* **2008**, *81*, 1377–1392.
- [24] L. Weber, H. B. Wartig, H.-G. Stammmer, B. Neumann, *Organometallics* **2001**, *20*, 5248–5250.
- [25] L. Weber, H. B. Wartig, H.-G. Stammmer, B. Neumann, *Z. Anorg. Allg. Chem.* **2001**, *627*, 2663–2668.
- [26] L. Weber, I. Domke, W. Greschner, K. Miqueu, A. Chrostowska, P. Baylère, *Organometallics* **2005**, *24*, 5455–5463.
- [27] For examples of recent work on 1,3,2-diazaboroles, see a) T. Habereder, H. Nöth, *Appl. Organomet. Chem.* **2003**, *17*, 525–538; b) L. Weber, I. Domke, J. Kahlert, H.-G. Stammmer, *Eur. J. Inorg. Chem.* **2006**, 3419–3424; c) L. Weber, A. Rausch, H.-G. Stammmer, B. Neumann, *Z. Anorg. Allg. Chem.* **2004**, *630*, 2657–2664; d) L. Weber, J. Förster, H.-G. Stammmer, B. Neumann, *Eur. J. Inorg. Chem.* **2006**, 5048–5056; e) L. Weber, M. Schnieder, T. C. Maciel, H. B. Wartig, M. Schimmel, R. Boese, D. Bläser, *Organometallics* **2000**, *19*, 5791–5794; f) J. M. Murphy, J. D. Lawrence, K. Kawamura, C. Incarvito, J. F. Hartwig, *J. Am. Chem. Soc.* **2006**, *128*, 13684–13685; g) Y. Segawa, M. Yamashita, K. Nozaki, *Science* **2006**, *314*, 113–115; h) T. B. Marder, *Science* **2006**, *314*, 69–70; i) H. Braunschweig, *Angew. Chem.* **2007**, *119*, 1990–1992; *Angew. Chem. Int. Ed.* **2007**, *46*, 1946–1948; j) Y. Segawa, M. Yamashita, K. Nozaki, *Angew. Chem. Int. Ed.* **2007**, *46*, 6710–6713; k) T. Kajiwara, T. Terabayashi, M. Yamashita, K. Nozaki, *Angew. Chem.* **2008**, *120*, 6708–6712; *Angew. Chem. Int. Ed.* **2008**, *47*, 6606–6610; l) Y. Segawa, Y. Suzuki, M. Yamashita, K. Nozaki, *J. Am. Chem. Soc.* **2008**, *130*, 16069–16079; m) M. Yamashita, Y. Suzuki, Y. Segawa, K. Nozaki, *Chem. Lett.* **2008**, *37*, 802–803; n) T. Terabayashi, T. Kajiwara, M. Yamashita, K. Nozaki, *J. Am. Chem. Soc.* **2009**, *131*, 14162–14163; o) A. Hinchliffe, F. S. Mair, E. J. L. McInnes, R. G. Pritchard, J. E. Warren, *Dalton Trans.* **2008**, 222–233; p) E. Giziroglu, B. Donnadieu, G. Bertrand, *Inorg. Chem.* **2008**, *47*, 9751–9753; q) A. Chrostowska, M. Maciejczyk, A. Dargelos, P. Baylère, L. Weber, V. Werner, D. Eickhoff, H.-G. Stammmer, B. Neumann, *Organometallics* **2010**, *29*, 5192–5198; r) L. Weber, J. Halama, V. Werner, K. Hanke, L. Böhling, A. Chrostowska, A. Dargelos, M. Maciejczyk, A.-L. Raza, H.-G. Stammmer, B. Neumann, *Eur. J. Inorg. Chem.* **2010**, 5416–5425.
- [28] S. Maruyama, Y. Kawanishi, *J. Mater. Chem.* **2002**, *12*, 2245–2249.
- [29] L. Weber, I. Domke, C. Schmidt, T. Braun, H.-G. Stammmer, B. Neumann, *Dalton Trans.* **2006**, 2127–2132.
- [30] L. Weber, A. Penner, I. Domke, H.-G. Stammmer, B. Neumann, *Z. Anorg. Allg. Chem.* **2007**, *633*, 563–569.
- [31] L. Weber, D. Eickhoff, V. Werner, L. Böhling, S. Schwedler, A. Chrostowska, A. Dargelos, M. Maciejczyk, H.-G. Stammmer, B. Neumann, *Dalton Trans.* **2011**, *40*, 4434–4446.
- [32] S. Schwedler, D. Eickhoff, R. Brockhinke, D. Cherian, L. Weber, A. Brockhinke, *Phys. Chem. Chem. Phys.* **2011**, *13*, 9301–9310.
- [33] L. Weber, V. Werner, I. Domke, H.-G. Stammmer, B. Neumann, *Dalton Trans.* **2006**, 3777–3784.
- [34] L. Weber, V. Werner, M. A. Fox, T. B. Marder, S. Schwedler, A. Brockhinke, H.-G. Stammmer, B. Neumann, *Dalton Trans.* **2009**, 1339–1351.
- [35] L. Weber, V. Werner, M. A. Fox, T. B. Marder, S. Schwedler, A. Brockhinke, H.-G. Stammmer, B. Neumann, *Dalton Trans.* **2009**, 2823–2831.
- [36] L. Weber, J. Kahlert, H.-G. Stammmer, B. Neumann, *Z. Anorg. Allg. Chem.* **2008**, *634*, 1729–1734.
- [37] X. Y. Liu, D. R. Bai, S. Wang, *Angew. Chem.* **2006**, *118*, 5601–5604; *Angew. Chem. Int. Ed.* **2006**, *45*, 5475–5478.
- [38] A. Pelter, K. Smith, H. C. Brown, *Borane Reagents*, Academic Press London, **1988**, p. 428.
- [39] For examples of X-ray structures containing the BMes₂ group, see: a) K. Okada, T. Sugawa, M. Oda, *J. Chem. Soc. Chem. Commun.* **1992**, 74–75; b) S. M. Cornet, K. B. Dillon, C. D. Entwistle, M. A. Fox, A. E. Goeta, H. P. Goodwin, T. B. Marder, A. L. Thompson, *Dalton Trans.* **2003**, 4395–4405; c) C. D. Entwistle, A. S. Batsanov, J. A. K. Howard, M. A. Fox, T. B. Marder, *Chem. Commun.* **2004**, 702–703.
- [40] C. D. Entwistle, T. B. Marder, P. S. Smith, J. A. K. Howard, M. A. Fox, S. A. Mason, *J. Organomet. Chem.* **2003**, *680*, 165–173.
- [41] For examples of X-ray structures containing the BMes₂ group attached to para-phenylene rings see a) J. O. Huh, Y. Do, M. H. Lee, *Organometallics* **2008**, *27*, 1022–1025; b) J. O. Huh, H. Kim, K. M. Lee, Y. S. Lee, Y. Do, M. H. Lee, *Chem. Commun.* **2010**, *46*, 1138–1140, and, for example, references [6–8].
- [42] For examples of X-ray structures containing the BMes₂ group attached to 2-thiophene rings see references [11, 13h, 21].
- [43] A direct structural comparison between a BMes₂-para-phenylene and a BMes₂-2-thiophene is found in reference [12].
- [44] J. Fiedler, S. Zališ, A. Klein, F. M. Hornung, W. Kaim, *Inorg. Chem.* **1996**, *35*, 3039–3043; X-ray analysis of Mes₂BPh.
- [45] A. J. Mäkinen, I. G. Hill, M. Kinoshita, T. Noda, Y. Shirota, Z. H. Kafafi, *J. Appl. Phys.* **2002**, *91*, 5456–5461.
- [46] P. R. Jones, M. J. Drews, J. K. Johnson, P. S. Wong, *J. Am. Chem. Soc.* **1972**, *94*, 4595–4599.
- [47] A. Ronlán, J. Coleman, O. Hammerich, V. D. Parker, *J. Am. Chem. Soc.* **1974**, *96*, 845–849.
- [48] T. Yanai, D. P. Tew, N. C. Handy, *Chem. Phys. Lett.* **2004**, *393*, 51–57.
- [49] A. Dreuw, J. L. Weisman, M. Head-Gordon, *J. Chem. Phys.* **2003**, *119*, 2943–2946.
- [50] Y. Tawada, T. Tsuneda, S. Yanagisawa, T. Yanai, K. Hirao, *J. Chem. Phys.* **2004**, *120*, 8425–8433.
- [51] M. J. G. Peach, P. Benfield, T. Helgaker, D. J. Tozer, *J. Chem. Phys.* **2008**, *128*, 044118.
- [52] D. Jacquemin, E. A. Perpète, G. E. Scuseria, I. Ciofini, C. Adamo, *J. Chem. Theory Comput.* **2008**, *4*, 123–135.
- [53] T. Stein, L. Kronik, R. Baer, *J. Am. Chem. Soc.* **2009**, *131*, 2818–2820.
- [54] M. A. Rohrdanz, K. M. Martins, J. M. Herbert, *J. Chem. Phys.* **2009**, *130*, 054112.
- [55] M. J. G. Peach, C. R. L. Sueur, K. Ruud, M. Guillaume, D. J. Tozer, *Phys. Chem. Chem. Phys.* **2009**, *11*, 4465–4470.
- [56] A. D. Dwyer, D. J. Tozer, *Phys. Chem. Chem. Phys.* **2010**, *12*, 2816–2818.
- [57] E. Runge, E. K. U. Gross, *Phys. Rev. Lett.* **1984**, *52*, 997–1000.
- [58] M. E. Casida, in *Recent Advances in Density Functional Methods, Part I*, (Ed.: D. P. Chong), Singapore, World Scientific, **1995**, pp. 155–192.
- [59] P. Wiggins, J. A. G. Williams, D. J. Tozer, *J. Chem. Phys.* **2009**, *131*, 091101.

- [60] P. Bäuerle, F. Würthner, G. Götz, F. Effenberger, *Synthesis* **1993**, *11*, 1099–1103.
- [61] A. D. Becke, *J. Chem. Phys.* **1993**, *98*, 5648–5652.
- [62] C. Lee, W. Yang, R. G. Parr, *Phys. Rev. B* **1988**, *37*, 785–789.
- [63] P. J. Stephens, F. J. Devlin, C. F. Chabalowski, M. J. Frisch, *J. Phys. Chem.* **1994**, *98*, 11623–11627.
- [64] a) G. A. Petersson, M. A. Al-Laham, *J. Chem. Phys.* **1991**, *94*, 6081; b) G. A. Petersson, A. Bennett, T. G. Tensfeldt, M. A. Al-Laham, W. A. Shirley, J. Mantzaris, *J. Chem. Phys.* **1988**, *89*, 2193.
- [65] Gaussian 03, Revision C.02, M. J. Frisch, G. W. Trucks, H. B. Schlegel, G. E. Scuseria, M. A. Robb, J. R. Cheeseman, J. A. Montgomery, Jr., T. Vreven, K. N. Kudin, J. C. Burant, J. M. Millam, S. S. Iyengar, J. Tomasi, V. Barone, B. Mennucci, M. Cossi, G. Scalmani, N. Rega, G. A. Petersson, H. Nakatsuji, M. Hada, M. Ehara, K. Toyota, R. Fukuda, J. Hasegawa, M. Ishida, T. Nakajima, Y. Honda, O. Kitao, H. Nakai, M. Klene, X. Li, J. E. Knox, H. P. Hratchian, J. B. Cross, C. Adamo, J. Jaramillo, R. Gomperts, R. E. Stratmann, O. Yazyev, A. J. Austin, R. Cammi, C. Pomelli, J. W. Ochterski, P. Y. Ayala, K. Morokuma, G. A. Voth, P. Salvador, J. J. Dannenberg, V. G. Zakrzewski, S. Dapprich, A. D. Daniels, M. C. Strain, O. Farkas, D. K. Malick, A. D. Rabuck, K. Raghavachari, J. B. Foresman, J. V. Ortiz, Q. Cui, A. G. Baboul, S. Clifford, J. Cioslowski, B. B. Stefanov, G. Liu, A. Liashenko, P. Piskorz, I. Komaromi, R. L. Martin, D. J. Fox, T. Keith, M. A. Al-Laham, C. Y. Peng, A. Nanayakkara, M. Challacombe, P. M. W. Gill, B. Johnson, W. Chen, M. W. Wong, C. Gonzalez, J. A. Pople, Gaussian, Inc., Wallingford CT, **2004**.
- [66] Gaussian 09, Revision A.02, M. J. Frisch, G. W. Trucks, H. B. Schlegel, G. E. Scuseria, M. A. Robb, J. R. Cheeseman, G. Scalmani, V. Barone, B. Mennucci, G. A. Petersson, H. Nakatsuji, M. Caricato, X. Li, H. P. Hratchian, A. F. Izmaylov, J. Bloino, G. Zheng, J. L. Sonnenberg, M. Hada, M. Ehara, K. Toyota, R. Fukuda, J. Hasegawa, M. Ishida, T. Nakajima, Y. Honda, O. Kitao, H. Nakai, T. Vreven, J. A. Montgomery, Jr., J. E. Peralta, F. Ogliaro, M. Bearpark, J. J. Heyd, E. Brothers, K. N. Kudin, V. N. Staroverov, R. Kobayashi, J. Normand, K. Raghavachari, A. Rendell, J. C. Burant, S. S. Iyengar, J. Tomasi, M. Cossi, N. Rega, J. M. Millam, M. Klene, J. E. Knox, J. B. Cross, V. Bakken, C. Adamo, J. Jaramillo, R. Gomperts, R. E. Stratmann, O. Yazyev, A. J. Austin, R. Cammi, C. Pomelli, J. W. Ochterski, R. L. Martin, K. Morokuma, V. G. Zakrzewski, G. A. Voth, P. Salvador, J. J. Dannenberg, S. Dapprich, A. D. Daniels, O. Farkas, J. B. Foresman, J. V. Ortiz, J. Cioslowski, D. J. Fox, Gaussian, Inc., Wallingford CT, **2009**.
- [67] A. R. Allouche, Gabedit 2.1.0, CNRS et Université Claude Bernard Lyon1, **2007**. Available at <http://gabedit.sourceforge.net>.
- [68] N. M. O'Boyle, A. L. Tenderholt, K. M. Langner, *J. Comput. Chem.* **2008**, *29*, 839–845.
- [69] A short history of “SHELX”. G. M. Sheldrick, *Acta Crystallogr. Sect. A* **2008**, *64*, 112–122.

Received: July 5, 2011

Published online: December 30, 2011